Characterization of Anisotropic Aluminum Magnetic Shielding Tensors. Distorted Octahedral Complexes and Linear Molecules

Robert W. Schurko,[†] Roderick E. Wasylishen,*[,†] and Hans Foerster[‡]

Department of Chemistry, Dalhousie University, Halifax, Nova Scotia, B3H 4J3 Canada, and Bruker Analytik GmbH, Application Laboratory, D-76287 Rheinstetten, Germany

Received: May 26, 1998; In Final Form: July 31, 1998

The orientation dependence of aluminum chemical shielding is shown to vary from a few ppm in distorted octahedral complexes to more than 400 ppm in linear molecules. The analysis of solid-state ^{27}Al NMR spectra of tris(acetylacetonato)aluminum(III), Al(acac)$_3$, and tris(tropolonato)aluminum(III), Al(trop)$_3$, obtained at three different applied magnetic fields (4.7, 9.4, and 18.8 T) reveal small ^{27}Al chemical shielding anisotropies of 3.8(3) and 9.0(3) ppm, respectively. Similarly, analysis of solid-state ^{27}Al NMR spectra of tris(2,2,6,6-tetramethyl-3,5-heptanedionato)-aluminum(III), Al(TMHD)$_3$, at 4.7 and 9.4 T yield an ^{27}Al chemical shielding anisotropy of 6.7(5) ppm. Aluminum nuclear quadrupole coupling constants, asymmetry parameters, and the relative orientations of the chemical shielding (CS) and electric field gradient (EFG) tensors are also reported. The utility of obtaining and analyzing solid-state NMR spectra at high applied magnetic field strengths is demonstrated. Aluminum nuclear spin-rotation constants available from recent high-resolution Fourier transform microwave spectroscopy studies of aluminum(I) isocyanide (AlNC) and aluminum(I) chloride (AlCl) indicate large ^{27}Al CS anisotropies of 406(9) and 477(17) ppm, respectively. Experimental results are compared with theoretically-calculated CS and EFG parameters, using both restricted Hartree−Fock methods and density functional theory.

Introduction

The aluminum-27 nucleus (nuclear spin $I = 5/2$) is well-suited for solid-state NMR studies,[1] due to its high natural abundance (100%), relatively large magnetic moment, and small nuclear quadrupole moment.[2] It is possible to easily obtain and analyze solid-state ^{27}Al magic-angle spinning (MAS) NMR spectra of a variety of materials since the central transition (1/2 ↔ −1/2) is dependent only upon the second-order quadrupolar interaction and the isotropic chemical shift.[1] Solid-state ^{27}Al NMR has especially found use in materials science for the study of a variety of substances including zeolites, ceramics, cements, and glasses.[1,3−5] Numerous isotropic ^{27}Al chemical shifts have been reported, indicating a chemical shift range of ca. 300 ppm.[6,7] In contrast, there are very few reports of ^{27}Al chemical shielding anisotropy (CSA) in the literature. Samoson and co-workers reported the first evidence of ^{27}Al CSA in a study of trialuminum tris(orthophosphate) hydrate, $AlPO_4$-21, which contains one tetrahedral and two pentacoordinate aluminum sites.[8] They found that it was difficult to simulate NMR spectra of the pentacoordinate sites without including orientation-dependent chemical shifts; however, the overlap of signals arising from chemically distinct sites rendered an exact determination of the magnitude of the CSA impossible. Recently, Vosegaard and Jakobsen reported aluminum CSA in sapphire (α-Al_2O_3).[9] From single-crystal ^{27}Al NMR experiments, they were able to determine the magnitude of the CSA as well as the orientations of the aluminum chemical shielding (CS) and electric field gradient (EFG) tensors in the molecular frame. At the same time, our group had submitted a report of a relatively large ^{27}Al CSA in aluminum trichloride phosphoryl trichloride, $AlCl_3$·$OPCl_3$.[10] Aside from these examples of aluminum CSA, the only other interaction that influences the line shape of solid-state NMR spectra in a similar fashion is the Knight shift,[11] which has been observed in the ^{27}Al NMR spectra of binary aluminum−metal alloys.[12] However, the Knight shift is only functional in conducting or semiconducting materials.

SCHEME 1

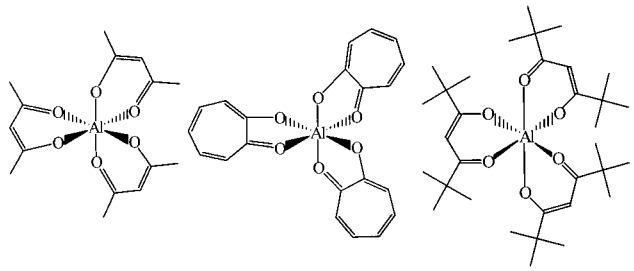

This paper reports several new examples of ^{27}Al CSA characteristic of two extremes—small values in pseudo-octahedral complexes and relatively large values in diatomic and linear triatomic molecules. In the first part of this paper, the small ^{27}Al CSAs observed in the octahedrally coordinated aluminum complexes tris(acetylacetonato)aluminum(III), Al(acac)$_3$, tris(tropolonato)aluminum(III), Al(trop)$_3$, and tris(2,2,6,6-tetramethyl-3,5-heptanedionato)aluminum(III), Al(TMHD)$_3$, are discussed (see Scheme 1). A comparison of known ^{27}Al CS tensors obtained from solid-state NMR experiments is given in Table 1. In the second part of the paper, known ^{27}Al nuclear spin-rotation constants obtained for alumi-

* Address correspondence to this author. Phone: 902-494-2564. Fax: 902-494-1310. E-mail: Rodw@is.dal.ca.
[†] Dalhousie University.
[‡] Bruker Analytik GmbH.

10.1021/jp982367k CCC: $15.00
Published on Web 11/03/1998

TABLE 1: Tabulation of Experimental Quadrupolar and Chemical Shift Data Obtained from NMR Experiments on Complexes Exhibiting Aluminum Chemical Shielding Anisotropy[a]

	quadrupolar parameters[b]		chemical shift parameters			Euler angles (deg)[c]			
complex	C_Q (MHz)	η	δ_{iso} (ppm)[d]	Ω (ppm)	κ	α	β	γ	ref
$AlPO_4-21$	7.35	0.5	15.8	44	0.64	90	70	90	8
(site 1,2)[e]	5.8	0.7	14.2						
sapphire, α-Al_2O_3	2.403(15)	0.01(1)	18.8(3)	17.5(6)	0.96(4)	0	2.7	0	9
$AlCl_3 \cdot OPCl_3$	6.0(1)	0.15(1)	88(1)	60(1)	−0.70(2)	90	90	0	10
$Al(acac)_3$	3.03(1)	0.15(1)	0.0(3)	3.8(3)	0.70(3)	90	90	0	this work
$Al(trop)_3$	4.43(1)	0.08(2)	36.6(2)	9.0(3)	−0.25(5)	90	81	7	this work
$Al(TMHD)_3$	3.23(2)	0.10(1)	1.5(3)	6.7(5)	0.4(1)	90	90	0	this work

[a] Errors are given in parentheses. [b] Principal components of the EFG tensor: $|V_{11}| \leq |V_{22}| \leq |V_{33}|$. $C_Q = e^2qQ/h = eQV_{33}/h$. $\eta = (V_{11} - V_{22})/V_{33}$. [c] Errors in Euler angles given in text. [d] $\delta_{iso} = (\delta_{11} + \delta_{22} + \delta_{33})/3$. Referenced with respect to an external sample of 0.1 M $Al(NO_3)_3$(aq), $\delta_{iso}(^{27}Al)$ of $Al(H_2O)_6^{3+} = 0$ ppm. [e] No errors quoted, accurate simulations of spectra not possible (see text).

num(I) isocyanide, AlNC,[13,14] and aluminum(I) chloride, AlCl,[15] are utilized to determine the ^{27}Al CS tensor parameters for these molecules. It is interesting to note that the spans of these CS tensors ($\Omega > 400$ ppm, vide infra) are comparable to the entire ^{27}Al CS range.

Only a handful of ab initio calculations of ^{27}Al chemical shieldings have appeared in the literature,[16] with only two papers reporting ^{27}Al CS tensors.[10,17] Comparison of experimentally determined and theoretically calculated CS and EFG tensors provides information on the orientations of these tensors in the molecular frame as well as acting as a rigorous test of modern computational methods. We report theoretical ^{27}Al CS tensors and quadrupolar parameters calculated using restricted Hartree−Fock (RHF) methods and density functional theory (DFT) for $Al(acac)_3$, $Al(trop)_3$, AlNC, and AlCl as well as for several other simple systems.

Experimental Section

Tris(acetylacetonato)aluminum(III) (IUPAC name: tris(2,4-pentanedionato-*O*,*O*′)aluminum) and tris(2,2,6,6-tetramethyl-3,5-heptanedionato)aluminum(III), both 99.5% pure, were obtained from Aldrich and used without any further purification. Tris-(tropolonato)aluminum (III) (IUPAC name: tris(2-hydroxybenzaldehydato-*O*,*O*′)aluminum) was synthesized according to a procedure in the literature[18] and recrystallized from methanol.

Solid-state ^{27}Al NMR spectra were acquired at 4.7, 9.4, and 18.8 T ($\nu_0(^{27}Al) = 52.13$, 104.26 and 208.49 MHz) on Bruker MSL-200, AMX-400, and DSX-800 NMR spectrometers, respectively. MAS NMR spectra were acquired with samples at spinning speeds ranging from 4.0 to 10.5 kHz, with the accumulation of 256−2048 scans. For stationary samples, 1000−20000 transients were accumulated. All spectra were acquired with single-pulse experiments with the application of high-power proton decoupling. Pulse widths and relaxation delays were 1.0 μs and 2−4 s, respectively. Spectra were referenced with respect to 0.1 M $Al(NO_3)_3$(aq), where $Al(H_2O)_6^{3+}$(aq) has $\delta(^{27}Al) = 0.0$ ppm. The aqueous standard was also used to determine the 90° pulse for ^{27}Al (3.5 μs, $\nu_{rf} \simeq 70$ kHz) and set to 1.0 μs for the solid samples. Pre-acquisition delays of 10−40 μs were applied. Aluminum NMR spectral simulations were performed on an IBM-compatible PC (Pentium) using the WSOLIDS software package, which was developed in this laboratory. This software incorporates the space-tiling method of Alderman and co-workers for the generation of solid-state NMR powder patterns.[19]

RHF and DFT calculations of CS tensors and RHF, DFT, and MP2 calculations of EFG tensors were carried out on an IBM RISC 6000 Station using Gaussian 94.[20] Both 6-31G* and 6-311G* basis sets were implemented in the calculations, with the 6-31G** and 6-311G** basis sets employed for calculations on AlH and AlH_4^-. Chemical shielding calculations were performed using the gauge-including atomic orbital (GIAO) method.[21] DFT calculations utilized Becke's three parameter hybrid[22] and the correlation functional of Lee et al.[23] (i.e., B3LYP DFT calculations). Geometry optimizations of AlNC, AlCl, and several other diatomic systems were carried out at both RHF and MP2 levels of theory using the 6-311G*-(*) basis set. Since there is no established absolute chemical shielding scale for ^{27}Al, calculated ^{27}Al chemical shifts were referenced with respect to AlH_4^-, which has a calculated chemical shielding of $\sigma_{iso}(Al) = 512$ ppm[16d] and a measured chemical shift of $\delta_{iso}(^{27}Al) = 101$ ppm with respect to the standard $Al(H_2O)_6^{3+}$(aq).[24] Incidentally, Farrar and co-workers recently reported a calculation of $\sigma_{iso}(Al) = 612$ ppm for $Al(H_2O)_6^{3+}$ that gives a calculated chemical shift difference of 100 ppm,[16a] in excellent agreement with the experimentally determined difference in chemical shielding.[25] Calculated EFG tensors were converted from atomic units (au) to MHz[26] by multiplying the largest component of the EFG tensor, V_{33}, by $eQ/h \times 9.7177 \times 10^{21}$ V m^{-2}, where $Q(^{27}Al) = 1.403 \times 10^{-29}$ m^2 (ref 2).

Results and Discussion

Aluminum-27 MAS NMR of $Al(acac)_3$, $Al(trop)_3$, and $Al(TMHD)_3$. The NMR Hamiltonian for an isolated quadrupolar (spin $S > 1/2$) nucleus can be written as

$$H = H_Z + H_Q + H_{CS} \quad (1)$$

In moderate applied magnetic fields, the quadrupolar and CS Hamiltonians can be treated as perturbations on the Zeeman Hamiltonian. Under conditions of fast magic-angle spinning,[27] anisotropic CS interactions become negligible, and the line shape of the central transition ($1/2 \leftrightarrow -1/2$) of the quadrupolar nucleus is therefore dependent only upon the second-order quadrupolar interaction.[28] Accordingly, the position and line shape of the central transition are dependent only upon three parameters: the magnitude of the nuclear quadrupole coupling constant, C_Q; the quadrupolar asymmetry parameter, η; and the isotropic chemical shift, δ_{iso}. Expressions for calculating the central transition may be found in the original literature[28] as well as in several review articles.[29−31]

Aluminum-27 MAS NMR spectra were obtained for $Al(acac)_3$ and $Al(trop)_3$ at 9.4 (Figure 1) and 18.8 T, and analysis of these spectra yielded the quadrupolar parameters and isotropic chemical shifts listed in Table 1. The uncertainties in C_Q, η, and δ_{iso} (given in parentheses) were estimated by visual comparison of experimental and calculated spectra. The results for $Al(acac)_3$ are in excellent agreement with previously reported values ($C_Q = 3.0$ MHz and $\eta = 0.15$ (ref 32) and $C_Q = 2.85$ MHz and η

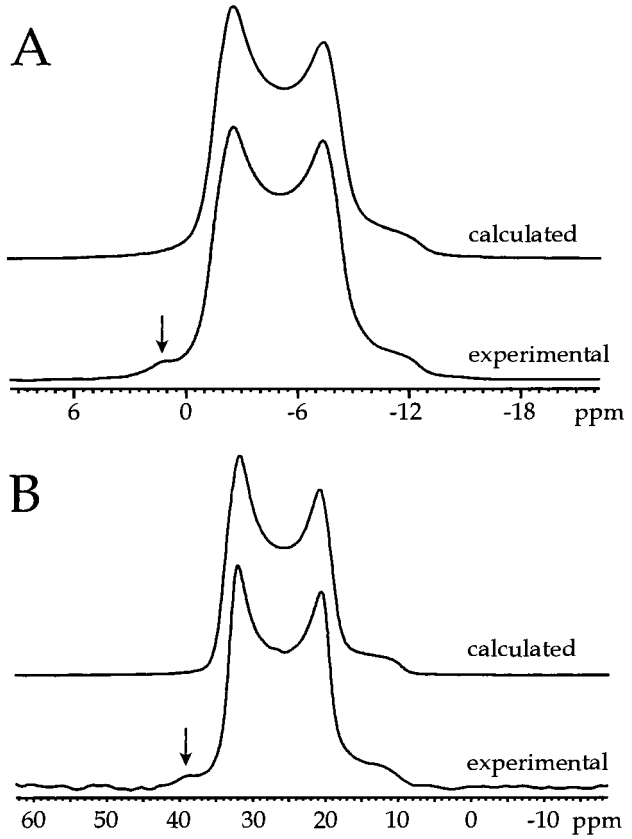

Figure 1. Experimental and calculated ^{27}Al MAS NMR spectra of the central transitions ($1/2 \leftrightarrow -1/2$) of (A) Al(acac)$_3$, $\nu_{rot} = 7853$ Hz, and (B) Al(trop)$_3$, $\nu_{rot} = 9955$ Hz, acquired at 9.4 T ($\nu_0(^{27}\text{Al}) = 104.26$ MHz). Evidence of the ($\pm 3/2 \leftrightarrow \pm 1/2$) satellite transitions are also visible and marked with arrows.

$\simeq 0$ (ref 33)). The former data were obtained from ^{27}Al MAS NMR spectra, while the latter were estimated from solid-state ^{27}Al spectra of stationary samples acquired at 2.35 T. Values of C_Q and η for Al(TMHD)$_3$ were obtained from the analysis of ^{27}Al NMR spectra acquired at 4.7 and 9.4 T (see Table 1).

Al(acac)$_3$ and Al(TMHD)$_3$ are both tris(β-ketoenolato) complexes,[34] with the oxygen atoms positioned in an octahedral arrangement about the central aluminum atom. As isolated molecules, these complexes possess D_3 symmetry, with each of the three diketo ligands forming a six-membered chelate ring with the aluminum. Due to the similar structural environments about the aluminum centers, the $C_Q(^{27}\text{Al})$ and $\delta_{iso}(^{27}\text{Al})$ of Al(acac)$_3$ and Al(TMHD)$_3$ are of comparable magnitudes. The tropolonato ions in Al(trop)$_3$ form five-membered chelate rings with the aluminum, and the interoxygen distances are reduced[35] in comparison to the six-membered chelate ring of Al(acac)$_3$.[36] This leads to the oxygen atoms adopting a distorted octahedral arrangement, which gives rise to augmented electric field gradients at the aluminum. As a result, the magnitude of C_Q in Al(trop)$_3$ is markedly larger than that observed in the former compounds. The isotropic aluminum chemical shift is also very sensitive to changes in structure, as demonstrated by the deshielding of the aluminum nucleus by ca. 35 ppm as compared to the six-membered chelate ring complexes.

Solid-State ^{27}Al NMR in Stationary Samples. *Theoretical Background.* In analyzing the NMR spectra of solid stationary samples, the effects of CSA on line shape must be considered. There are many examples in the literature in which the CS and EFG tensor parameters have been extracted through analyses of powder NMR spectra of stationary samples;[37−41] correspondingly, the treatment of the problem is well known and will not be discussed in detail here.

The chemical shielding interaction is described by a second-rank tensor with principal components defined from least to most shielded as $\sigma_{11} \leq \sigma_{22} \leq \sigma_{33}$. The corresponding chemical shift principal components (i.e., chemical shielding with respect to some reference sample) are defined from least to most shielded as $\delta_{11} \geq \delta_{22} \geq \delta_{33}$. Depending on the convention used, the term chemical shielding anisotropy may have different meanings.[42,43] In our recent work, we have taken the CSA to be synonymous with the span of the CS tensor, Ω, which is defined as[42]

$$\Omega = \delta_{11} - \delta_{33} = \sigma_{33} - \sigma_{11} \tag{2}$$

Furthermore, the shape of the spectrum is described by the skew, κ, which is defined as[42]

$$\kappa = 3(\delta_{22} - \delta_{iso})/\Omega = 3(\sigma_{iso} - \sigma_{22})/\Omega \tag{3}$$

where $+1 \geq \kappa \geq -1$.

The relative orientation of the EFG and CS PASs are described such that the orientation of the CS tensor in the EFG PAS is defined by three Euler angles (α, β and γ), and the following rotational operation:[44]

$$R(\alpha,\beta,\gamma) = R_{Z''}(\gamma)R_{Y'}(\beta)R_Z(\alpha) \tag{4}$$

The frequencies of the spectrum of the central transition can be calculated from

$$\nu_{1/2\leftrightarrow -1/2} = \nu_0 + \nu_Q^{(2)}(\theta,\phi) - \nu_{CS}(\theta,\phi,\alpha,\beta,\gamma) \tag{5}$$

where ν_0 is the Larmor frequency, $\nu_Q^{(2)}$ is the second-order quadrupolar frequency shift, and ν_{CS} is the orientation-dependent chemical shift frequency as defined previously.[45] The polar angles θ and ϕ describe the orientation of the EFG PAS with respect to the applied magnetic field. Powder patterns are simulated by calculating frequencies over a large number of angles, θ and ϕ.[19] The stationary NMR spectrum of the central transition of a quadrupolar nucleus can be computed from the knowledge of eight parameters: the quadrupolar parameters, C_Q and η; the CS parameters, δ_{iso}, Ω, and κ; and the Euler angles α, β, and γ.

The majority of publications concerning solid-state ^{27}Al NMR involve materials and complexes possessing tetrahedrally and octahedrally oxygen-coordinated aluminum centers.[1,7,46] In many cases, the materials investigated are disordered solids, or there are multiple aluminum sites present; consequently, broad and/or overlapping powder patterns make it very difficult to extract CS tensor information from the spectra. Al(acac)$_3$ and Al(trop)$_3$ are ideal compounds to study since known crystal structures[35,36] reveal that (i) there is nearly octahedral symmetry about the aluminum centers and (ii) there is only one crystallographically distinct aluminum nucleus per unit cell. In addition, both complexes have approximate C_3 and C_2 rotation axes that are normal to one another, where one might expect that principal components of the EFG and CS tensors would be directed.[47−49] For example, in the case of Co(acac)$_3$, single-crystal ^{59}Co NMR measurements indicate that the unique principal components of the cobalt CS and EFG tensors are close to the local C_3 axis.[49] Although there is no report of the crystal structure of Al(TMHD)$_3$ in the literature, it is clear from the ^{27}Al NMR results (vide infra) that the aluminum is hexacoordinate with pseudo-octahedral symmetry.

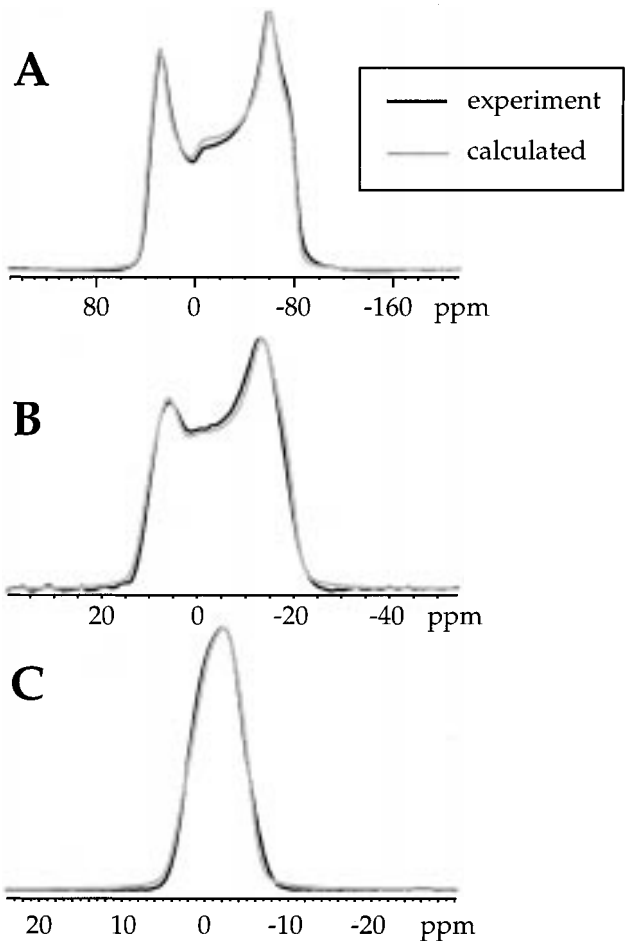

Figure 2. Experimental and calculated solid-state ^{27}Al NMR spectra of stationary samples of Al(acac)$_3$ at (A) 4.7, (B) 9.4, and (C) 18.8 T. See Table 1 for simulation parameters.

Al(acac)$_3$. Solid-state ^{27}Al NMR spectra of stationary samples of Al(acac)$_3$ at three different fields are pictured in Figure 2 along with the calculated spectra. Analyses of these spectra were completed with the following parameters: $C_Q(^{27}Al) = 3.03(1)$ MHz, $\eta = 0.15(1)$, $\delta_{iso} = 0.0(3)$ ppm, $\Omega = 3.8(3)$ ppm, and $\kappa = 0.70(3)$. Agreement between experimental and calculated spectra at all fields is quite good. Values of C_Q, η, and δ_{iso} obtained from MAS NMR spectra were fixed, and the remaining parameters were varied until best fits were obtained at all three fields. Uncertainties in spectral parameters were estimated by visual comparison of experimental and calculated spectra. The relative orientation of the EFG and CS tensors is given by the Euler angles $\alpha = 90°(\pm 15°)$, $\beta = 90°(\pm 10°)$, and $\gamma = 0°(\pm 30°)$, which sets the least shielded component of the CS tensor, δ_{11}, along the direction of the largest component of the EFG tensor, V_{33}; δ_{22} along V_{11}; and δ_{33} along V_{22}. Since δ_{11} and δ_{22} are very close to one another, altering the value of γ does not result in significant changes in the shape of the central transition. Consequently, the error in γ is significantly larger in comparison to the errors in α and β. The span of the shielding tensor is very small; however, comparison of experimental and calculated spectra (with and without the CSA) reveal that there is clearly a CSA effect present on the ^{27}Al NMR line shape (see Figure 3).

In many cases, single-crystal NMR studies have been used to elicit information on the orientation of NMR interaction tensors in the frame of the molecule.[47,50−53] When suitable single crystals are unavailable and only powder NMR spectra can be obtained, it is sometimes possible to utilize (i) molecular symmetry and/or (ii) theoretical CS or EFG tensors to predict the orientation of the interaction tensors in the molecule. The aluminum EFG tensor of Al(acac)$_3$ has near-axial symmetry ($\eta = 0.15$), which indicates that V_{33} is the quasi-unique component, and the value of the skew, $\kappa = 0.7$, signifies that the CS tensor is also almost axially symmetric, with δ_{33} as the quasi-unique component. Note that the term quasi-unique is used to describe a single principal component that is distinctly separated from the other two components which are of similar magnitude for tensors that are close to being axially symmetric. On the basis of the roughly axially symmetric interaction tensors and the relative orientation of the EFG and CS frames, two possible orientations of the interaction tensors with respect to the molecular frame are suggested. One possible orientation has V_{33} (the quasi-unique EFG principal component) oriented near or along the direction of the approximate C_3 axis, which positions δ_{11} near or along this axis as well. The other possibility has the most shielded principal component, δ_{33}, aligned near the C_3 axis, placing V_{22} along this direction as well. In both cases, one set of remaining principal components would be directed along or near one of the three C_2 symmetry axes present in the molecule.

One might expect to find both of the quasi-unique components of the EFG and CS tensors (i.e., V_{33} and δ_{33}) aligned along the C_3 symmetry axis. However, calculated spectra incorporating these tensor orientations indicate that this is not the case. The EFG is a ground-state first-order property, predominantly dependent upon the arrangement of nearest neighbors about the central nucleus, whereas CS is a second-order property, dependent upon the virtual as well as the ground electronic states of the molecule.[54] In addition, the magnitude of the ^{27}Al CSA is very small on the overall shielding scale of ^{27}Al, whereas the ^{27}Al C_Q is of small to moderate magnitude (small values of $C_Q(^{27}Al)$ range from 0.3−0.6 MHz in alums,[46,55] to values on the order of 25−45 MHz in monomeric and dimeric organoaluminum compounds).[56] Therefore, the orientation of the quasi-unique component of the EFG tensor should be dictated by molecular symmetry, whereas the CS tensor orientation is somewhat more ambiguous, predominantly due to the small value of the CSA. From these arguments, it is proposed that the most probable orientation of the EFG and CS tensors in Al(acac)$_3$ is one in which V_{33} and δ_{11} are along or near the C_3 symmetry axis. No additional information can be gained from experimental data regarding the orientation of the remaining principal components with respect to the molecular frame; however, we reiterate that from the Euler angles and the crystal structure of Al(acac)$_3$ it is known that δ_{22} is oriented along or close to V_{11} and δ_{33} is near to V_{22} with one set of these components aligned in the direction of one of the C_2 symmetry axes.

To further establish the orientation of the interaction tensors with respect to the molecular frame, it is worthwhile to compare theoretical CS and EFG tensor orientations with experimental results (see Table 2). The geometry of Al(acac)$_3$ used for the theoretical calculations was taken from the reported X-ray crystal study,[36] with carbon−hydrogen bond lengths optimized using RHF theory with the 6-311G** basis set.

Both RHF and DFT(B3LYP) CS calculations with 6-31G* and 6-311G* basis sets predict CSA at the aluminum nucleus. Several interesting observations can be made. The CS calculations carried out with the 6-31G* basis set are closest to the experimentally observed values, although the improved results with the smaller basis set are likely fortuitous. The RHF/6-31G* calculations predict a span of 3.1 ppm, which is quite

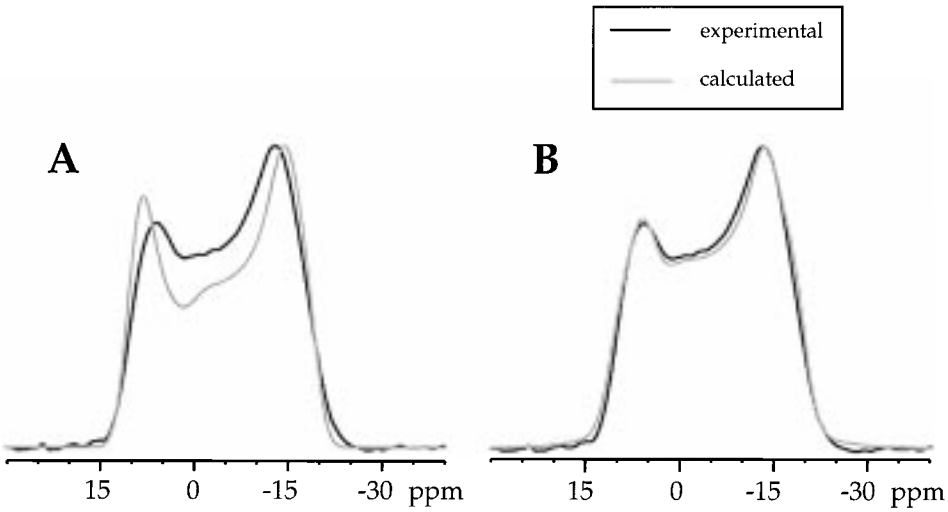

Figure 3. Experimental and calculated solid-state ^{27}Al NMR spectra of Al(acac)$_3$ at 9.4 T. In panel A, no CSA is included in the simulation, whereas in panel B, the CSA is included ($\Omega = 3.8$ ppm).

TABLE 2: Theoretically Calculated Chemical Shielding Tensors and Quadrupolar Parameters for Al(acac)$_3$ and Al(trop)$_3$

	quadrupolar parameters		chemical shielding principal components (ppm)			chemical shift principal components (ppm)[a]			chemical shift parameters		
complex	C_Q (MHz)	η	σ_{11}	σ_{22}	σ_{33}	δ_{11}	δ_{22}	δ_{33}	δ_{iso} (ppm)	Ω (ppm)	κ
Al(acac)$_3$, exptl	3.03	0.15				−1.5	0.9	−2.3	0.0	3.8	0.70
RHF/6-31G*	2.11	0.05	619.8	622.3	622.9	−6.8	−9.3	−9.9	−8.6	3.1	−0.63
B3LYP/6-31G*	2.30	0.03	595.9	597.1	597.7	17.1	15.9	15.3	16.1	1.8	−0.32
RHF/6-311G*	2.37	0.05	600.8	607.6	608.1	12.2	5.4	4.9	7.5	7.3	−0.87
B3LYP/6-311G*	2.85	0.04	567.4	573.8	574.4	45.6	39.2	38.6	41.1	7.0	−0.81
Al(trop)$_3$, exptl	4.43	0.08				41.5	35.9	32.5	36.6	9.0	−0.24
RHF/6-31G*	3.36	0.04	592.2	599.6	602.4	20.8	13.4	10.6	14.9	10.2	−0.44
B3LYP/6-31G*	3.40	0.03	563.4	565.4	569.8	49.6	47.6	43.3	46.8	6.4	0.38
RHF/6-311G*	3.31	0.10	566.1	576.3	580.1	46.9	36.7	32.9	38.8	14.0	−0.47
B3LYP/6-311G*	4.00	0.07	522.9	532.6	537.8	90.1	80.4	75.2	81.9	14.9	−0.29

[a] Calculated ^{27}Al chemical shifts are referenced as described in the Experimental Section.

close to the measured value of 3.8(3) ppm. The RHF and DFT 6-311G* calculations overestimate the span of the CS tensor by ca. 3 ppm or more. Both RHF and DFT calculations predict a negative skew, implying that δ_{11} is the quasi-unique principal CS tensor component, contrary to the experimental results. Both methods using the 6-31G* basis set underestimate C_Q by 0.8−0.9 MHz; however, calculations with the 6-311G* basis set (notably B3LYP) yield values of C_Q that are close to the experimentally determined C_Q. In all cases, the calculated η values indicate an EFG tensor of near-axial symmetry.

The most interesting feature of these calculations is the predicted orientations of the CS and EFG tensors in the molecular frame and relative to one another. RHF calculations using either the 6-31G* or 6-311G* basis set and B3LYP/6-311G* calculations yield orientations in which V_{33} and δ_{11} are between 6° and 7° apart, aligned approximately along the direction of the molecular C_3 axis, in agreement with the first set of proposed tensor orientations above. The relative orientation of EFG and CS tensors, for example, in the RHF/6-31G* calculations, is described by the Euler angles $\alpha = 88.3°$, $\beta = 87.9°$, and $\gamma = 6.8°$ with other calculations giving similar data. These results are very close to the experimental orientation [$\alpha = 90° \pm 15°$, $\beta = 90° \pm 10°$, and $\gamma = 0° \pm 30°$]. The orientations of the CS and EFG tensors in the molecular frame are pictured in Figure 4. Despite the fact that the theoretical orientations of the CS and EFG PASs are in agreement with experiment, there are some discrepancies in the orientations of the remaining components in the molecular frame depending on the type of basis set applied in the calculation. The RHF/6-31G* calculations place V_{11} and δ_{22} oriented approximately along a C_2 rotation axis, separated by 7.0°, with δ_{33} and V_{22} set 3.3° apart and normal to both symmetry axes. In contrast, both the RHF and B3LYP 6-311G* calculations set δ_{33} and V_{22} ca. 16° apart and near a C_2 axis, with V_{11} and δ_{22} normal to the rotational symmetry axes. It is not surprising that there is some discrepancy between calculations with different methods and basis sets in the orientation of CS and EFG tensors in the molecular frame, since the magnitude of the CSA is very small and the "nonunique" components are very close to one another. At this point, no conclusion can be drawn about which set of principal components lies along the direction of one of the C_2 symmetry axes, but the theoretical relative orientations of the EFG and CS tensors obtained from RHF/6-31G*, RHF/6-311G*, and B3LYP/6-311G* calculations are in reasonable agreement with the experimentally determined orientations. B3LYP/6-31G* calculations yield CS tensor orientations that do not correspond to those observed experimentally or obtained using other basis sets.

Al(TMHD)$_3$. Analyses of ^{27}Al NMR spectra of stationary samples of Al(TMHD)$_3$ at 4.7 and 9.4 T yielded the following parameters: $C_Q(^{27}\text{Al}) = 3.23(2)$ MHz, $\eta = 0.10(1)$, $\delta_{iso} = 1.5(3)$ ppm, $\Omega = 6.7(5)$ ppm, and $\kappa = 0.4(1)$ with Euler angles $\alpha = 90°(\pm 25°)$, $\beta = 90°(\pm 10°)$, and $\gamma = 0°(\pm 30°)$. The magnitudes of C_Q, Ω, and κ suggest that there is a slightly less symmetric environment about the central aluminum atom in comparison to Al(acac)$_3$. The relative orientation of the CS and EFG tensors is the same as in Al(acac)$_3$, which suggests that these tensors may be oriented in the molecular frame in a

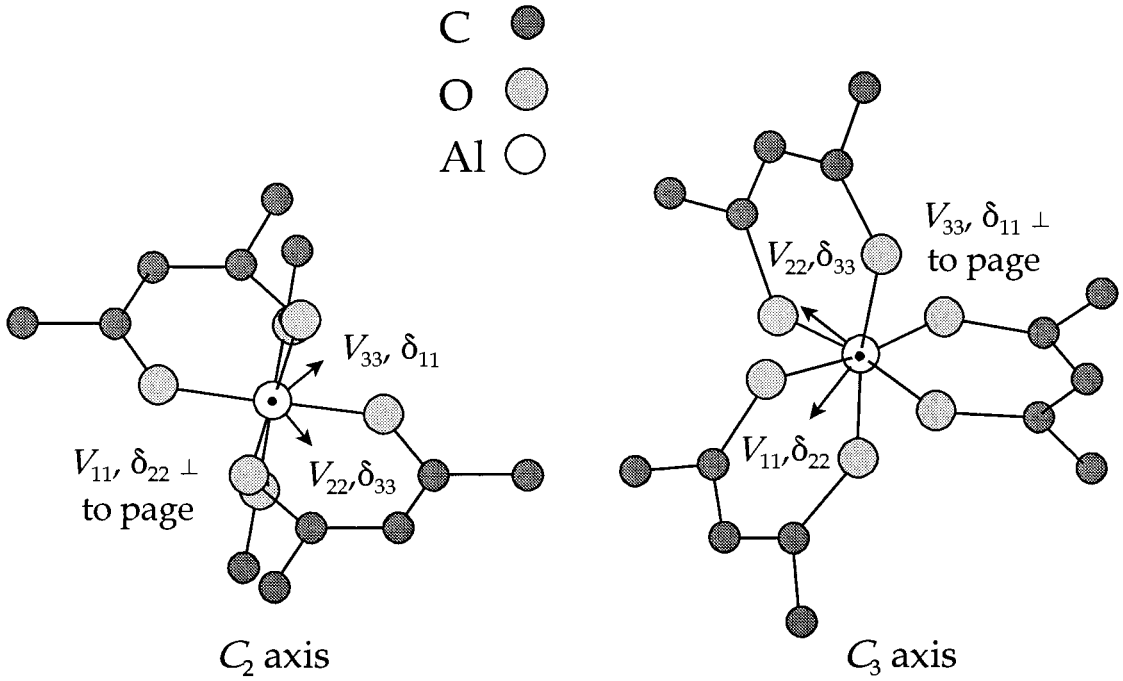

Figure 4. Two projections illustrating the orientations of the CS and EFG tensors in the molecular frame of Al(acac)$_3$ as determined by experimental and theoretical calculations (6-31G* basis set). V_{33} and δ_{11} are aligned along an approximate C_3 rotational axis, with V_{11} and δ_{22} roughly oriented with the C_2 symmetry axis.

manner similar to those in Al(acac)$_3$. The quoted errors in the CS parameters for Al(TMHD)$_3$ are slightly larger than those for Al(acac)$_3$ (or Al(trop)$_3$, vide infra) since spectra were not obtained and analyzed at 18.8 T where the effects of chemical shielding are more pronounced. Theoretical CS calculations were not carried out on Al(TMHD)$_3$ due to the absence of a reported crystal structure. Geometry optimization of such a large system would be time-consuming, but more importantly, since it would be performed on an isolated single molecule, it is unlikely to provide a reasonable representation of the geometry of the molecule in the solid state.

Al(trop)$_3$. Similar analyses were completed on the ^{27}Al NMR spectra of Al(trop)$_3$ with the following results: $C_Q(^{27}\text{Al}) = 4.43(1)$ MHz, $\eta = 0.08(2)$, $\delta_{iso} = 36.6(2)$ ppm, $\Omega = 9.0(3)$ ppm, and $\kappa = -0.25(5)$. Experimental and calculated spectra at three fields are presented in Figure 5, and a comparison of spectra with and without CSA is displayed in Figure 6. The larger CSA with respect to those in Al(acac)$_3$ and Al(TMHD)$_3$ and the nonaxial skew is presumably the result of diminished octahedral symmetry about the central aluminum nucleus (vide supra).[35,36] In addition to a near-C_3 symmetry axis, there is also a unique C_2 rotation axis positioned normal to the C_3 axis, resulting from the fact that two of the tropolone moieties are identical in terms of bond lengths, angles, and torsional angles with respect to the central aluminum nucleus. As in the case of Al(acac)$_3$, it is very likely that two principal components of each of the interaction tensors are aligned along the directions of these symmetry axes. The nonaxial CS tensor makes it difficult to assess which of the principal CS components may be aligned in the direction of the unique C_2 and approximate C_3 symmetry axes. However, the small quadrupolar asymmetry parameter ($\eta = 0.08$) once again indicates near-axial symmetry in the EFG tensor, which would strongly imply that V_{33} lies along or in the direction of the C_3 axis. The relative orientation of EFG and CS PASs in Al(trop)$_3$ are given by $\alpha = 90°(\pm 5°)$, $\beta = 81°(\pm 2°)$, and $\gamma = 7°(\pm 2°)$, setting δ_{11} at 9° off of the direction of V_{33} ; therefore, δ_{11} is the principal CS component that is situated near the approximate C_3 axis. The simulated spectra are sensitive to small changes in the Euler angles due to the increased magnitude of the CSA in Al(trop)$_3$; hence, the

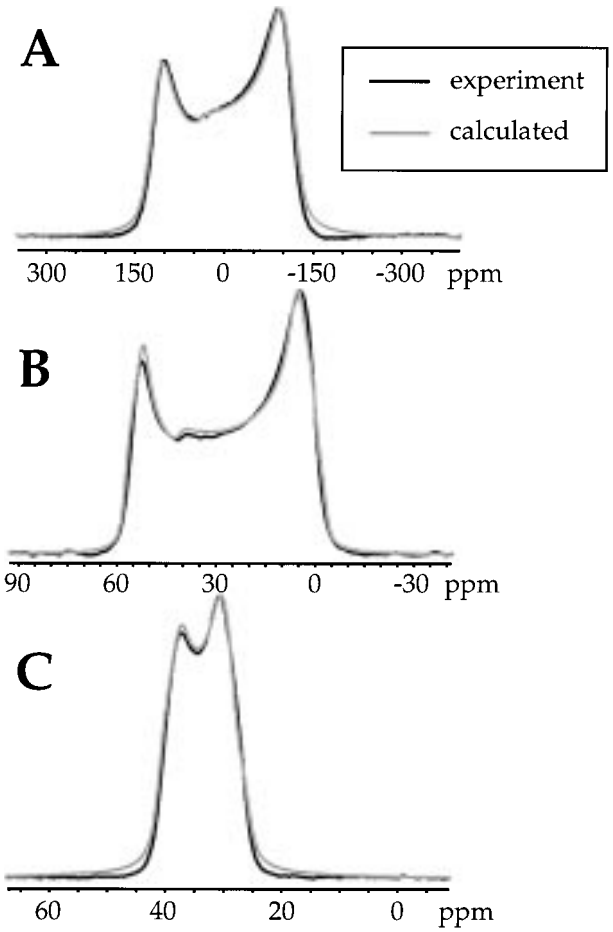

Figure 5. Experimental and calculated solid-state ^{27}Al NMR spectra of stationary samples of Al(trop)$_3$ at (A) 4.7, (B) 9.4, and (C) 18.8 T. See Table 1 for simulation parameters.

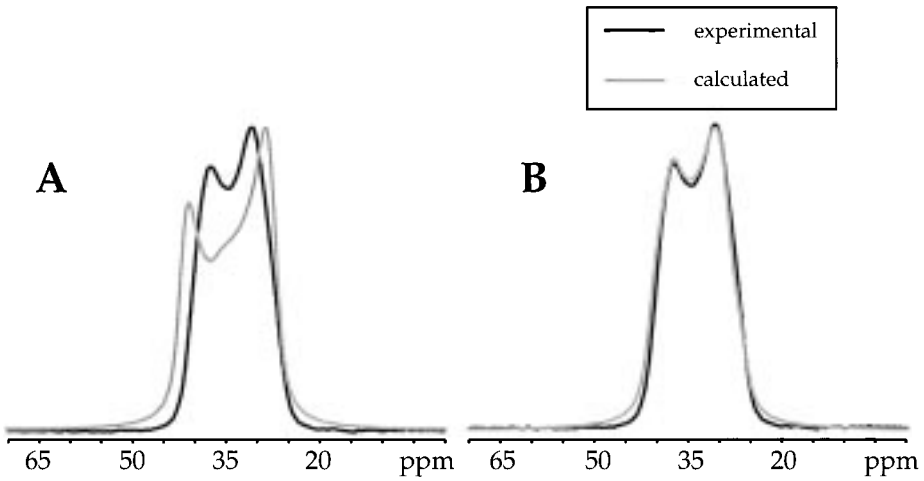

Figure 6. Experimental and calculated solid-state ^{27}Al NMR spectra of Al(trop)$_3$ at 18.8 T. (A) no CSA included, (B) with the CSA included (Ω = 9.0 ppm).

errors in the Euler angles are significantly smaller in comparison to those for Al(acac)$_3$ and Al(TMHD)$_3$. Again, no further information can be gained on the orientation of the other principal components relative to the molecular frame, except to say that one CS and EFG principal component should be aligned in the direction of the unique C_2 axis. The Euler angles reveal that, as in the case of Al(acac)$_3$, δ_{22} is oriented approximately in the direction of V_{11}, and δ_{33} is approximately along V_{22}.

Aluminum-27 CS tensors calculated using Hartree−Fock methods with the 6-31G* basis set are in very good agreement with the experimentally determined values—notably, the experimental and theoretical spans and skews are very close to one another (see Table 2). The B3LYP/DFT calculations with the same basis set underestimate the span considerably (ca. 3 ppm) and predict a skew of opposite sign. Calculations carried out using the larger 6-311G* basis set overestimate the span by 5 ppm or greater but also predict negative skews in accordance with experiment. All calculations predict deshielding at the ^{27}Al nucleus in Al(trop)$_3$ relative to Al(acac)$_3$, ranging from 20 to 40 ppm, which is in qualitative agreement with the measured deshielding of 36.6 ppm. The molecular geometry for the calculations was taken from crystal structure data,[35] with carbon−hydrogen bond lengths determined as described for Al(acac)$_3$. All calculations slightly underestimate the magnitude of C_Q, with B3LYP/6-311G* calculations predicting the asymmetry parameter quite accurately.

Several interesting results regarding the tensor orientations are extracted from these computations (see Figure 7). RHF/6-31G*, 6-311G*, and B3LYP/6-311G* calculations reveal that V_{33} and δ_{11} are in the direction of the near-C_3 axis and are 3.5−8.5° apart, in close agreement with our experimental results. However, the calculations place V_{11} and δ_{33} ca. 7.7(6)° from one another and place V_{22} and δ_{22} at ca. 2.0° apart, in contrast to the relative orientations of these components determined experimentally. Interestingly, the δ_{22} and V_{22} components fall along the direction of the unique C_2 axis (in agreement with our earlier suggestion), with V_{11} and δ_{33} normal to the two symmetry axes. In general, the theoretically calculated parameters are quite close to experimental values for Al(trop)$_3$, the only major discrepancy being the relative orientation of the CS and EFG tensors. Nevertheless, given that $V_{11} \approx V_{22}$, this is not a serious incongruity.

It is important to recognize that the theoretical calculations are generally carried out on an isolated molecule using a frozen geometry, while the experimental measurements are performed on a solid sample in which the molecular geometries are not rigid. Electric field gradients do not converge rapidly ($\sim r^{-3}$), and near-neighbor contributions can be significant.[57] Furthermore, there is growing evidence that post-Hartree−Fock calculations, which include electron correlation (e.g., second-order Møller−Plesset perturbation theory), and relativistic effects will be necessary to obtain better agreement between calculated and observed shielding[58] and EFG tensors.[59,60]

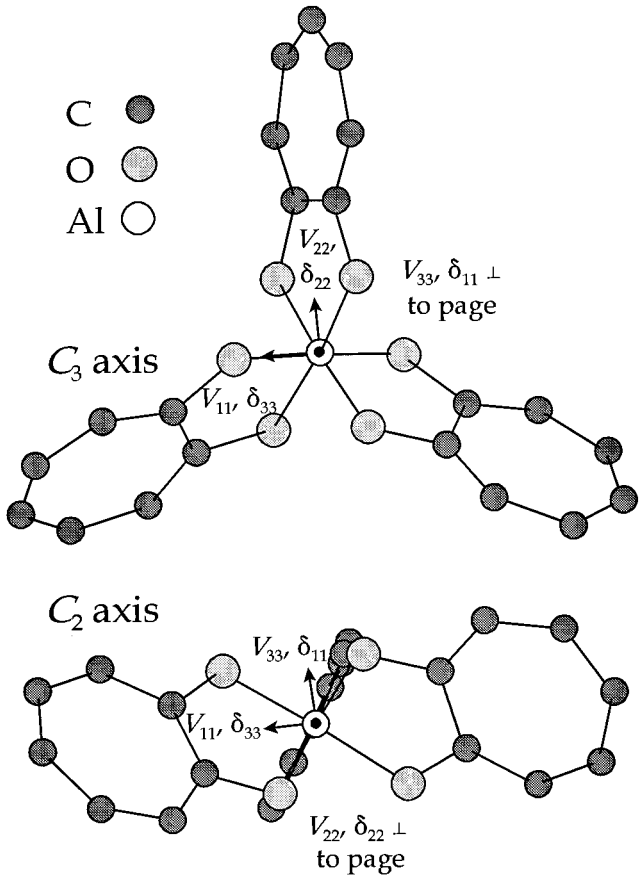

Figure 7. Two projections illustrating the orientations of the CS and EFG tensors in the molecular frame of Al(trop)$_3$ as determined by theoretical calculations. Theoretical calculations place V_{33} and δ_{11} along the unique C_3 symmetry axis, with V_{22} and δ_{22} along the direction of a C_2 symmetry axis.

Acquiring spectra at a number of different applied magnetic

fields is extremely useful in elucidating NMR parameters since the varying field dependence for CS and quadrupolar interactions produce differing spectral features and intensities. A single set of parameters extracted from spectral simulations are reliable if they yield best fit spectra at all applied magnetic field strengths. In several cases, theoretical CS and EFG relative orientations were tested in the reanalysis of the corresponding spectra. It was found that, despite relatively close fits at one applied magnetic field, the spectra could not be fit at all three fields. The acquisition of spectra on the high-field 18.8 T spectrometer (currently the highest field commercially available NMR spectrometer) is invaluable since the effects of a small CSA are very pronounced at the high field as opposed to the spectra acquired at 4.7 T. In contrast, the effects of the second-order quadrupolar interaction vary inversely with the applied field and are reduced by a factor of 4 on moving from 4.7 to 18.8 T.

Aluminum-27 Chemical Shielding Anisotropy in Linear Molecules. In practice, NMR spectroscopists measure chemical shifts that are related to differences in nuclear shieldings. Specifically, chemical shift is defined by[61]

$$\delta = (\nu_{\text{sample}} - \nu_{\text{ref}})/\nu_{\text{ref}} \times 10^6 \simeq \sigma_{\text{ref}} - \sigma_{\text{sample}} \quad (6)$$

where ν_{sample} and ν_{ref} are the resonance frequencies of the sample and the reference, respectively; σ_{ref} is the absolute chemical shielding of the reference compound; and σ_{sample} is the absolute shielding of the nucleus of interest in the sample. Absolute chemical shielding scales have been established for a number of elements using procedures outlined by Jameson[62] and Jameson and Mason.[61] As outlined below, it is possible to obtain chemical shielding data from the recently reported ^{27}Al nuclear spin-rotation constants, $C_\perp$, which have been obtained from high-resolution microwave spectroscopic studies of the linear molecules aluminum(I) isocyanide[14] and aluminum (I) chloride.[15] Because these are highly reactive molecules, it is impractical to measure experimental chemical shifts of other aluminum-containing compounds relative to AlCl or AlNC. Nevertheless, experimental data presented here serve as a benchmark for checking the reliability of theoretical calculations.

The chemical shielding tensor can be expressed according to the sum of the diamagnetic and the paramagnetic shielding tensors:[63]

$$\sigma = \sigma^{\text{d}} + \sigma^{\text{p}} \quad (7)$$

The diamagnetic shielding tensor is dependent only upon the ground electronic state of the molecule, while the paramagnetic term depends on both the ground- and excited-state molecular orbitals.

The difficulty in chemical shielding computations arises when calculating the paramagnetic shielding tensor, which involves excited-state molecular orbitals. Proper treatment of systems involving virtual states is improved by the inclusion of electron correlation;[58b,64] notwithstanding, due to the large computational times involved in performing such calculations, the majority of reported shielding calculations employ Hartree−Fock methods. Highly polarized basis sets are required to accurately calculate paramagnetic shielding contributions, and as a result, RHF theory often tends to overestimate the paramagnetic shielding component. Density functional theory implicitly includes electron correlation; however, the quality of the DFT calculation is largely dependent on the caliber of the correlation functional used in the calculation.[65] In the case of the Gaussian 94 suite of programs, the correlation functional utilized does not include any magnetic field dependence; therefore, it is not expected that the results of DFT chemical shielding calculations should be systematically "better" than the RHF calculations.[66]

The relationship between chemical shielding and nuclear spin-rotation tensors has been recognized for many years.[63,67] In the case of linear molecules

$$\sigma_\perp \simeq -\frac{m_{\text{p}}}{2mg_{\text{N}}}\frac{C_\perp}{B} + \sigma^{\text{d}}\,(\text{free atom}) \quad (8)$$

and

$$\sigma_{||} = \sigma_{||}^{\text{d}} \quad (9)$$

where m_{p} and m are the proton and electron masses, g_{N} is the nuclear g-factor (1.4565 for ^{27}Al), and B is the molecular rotational constant in Hz ($h/8\pi^2 I$). Values of σ^{d}(free atom) have been calculated for nuclei up to $Z = 86$ (ref 68) from ground-state atomic orbital wave functions. Accurate values of $\sigma_{||}^{\text{d}}$ are available from ab initio calculations. The sign preceding the first term of eq 8 is often written as positive;[62,67] however, the correct sign depends on the convention used for the sign of the nuclear spin-rotation constant.[69] Here we follow the sign convention of Gerry and co-workers.[69a] The most important point is that the first term of eq 8 is almost always negative.[69] Known exceptions are for the fluorine nuclei of ClF, BrF, IF, and SF_2.[70]

Consider the AlNC molecule, for which internuclear distances of r_{o}(Al,N) = 1.849 Å and r_{o}(N,C) = 1.171 Å[13] and a ^{27}Al spin-rotation constant of $C_\perp$ = 3.850(84) kHz[14] have been determined. From the above equations, one obtains $\sigma_{||} = 789.9$ ppm[68] and $\sigma_\perp$ = 384.3(8.9) ppm, for an isotropic chemical shielding of $\sigma_{\text{iso}} = (2\sigma_\perp + \sigma_{||})/3 = 519.5(9.0)$ ppm. The span of the chemical shielding tensor is given by $\Omega = \sigma_{||} - \sigma_\perp =$ 405.6(9.0) ppm. Similar calculations may be carried out for AlCl, which has r_e(Al,Cl) = 2.12983(1) Å[71] and $C_\perp$ = 5.54(16) kHz,[15] which gives $\sigma_{||}$ = 789.9 ppm and $\sigma_\perp$ = 313(17) ppm for σ_{iso} = 472(17) ppm and Ω = 477(17) ppm. These results are summarized and compared to theoretically calculated values in Table 3.

Theoretical GIAO NMR chemical shielding calculations were carried out on AlNC, AlCl, AlF, and AlH, using both experimentally determined molecular geometries[13,72,73] as well as theoretically optimized structures. There are several striking features in comparing the theoretical and experimental results in Table 3. For both AlNC and AlCl, the theoretical shielding parameters are in very good agreement with the experimental values, notably those calculated values obtained with the RHF and DFT methods using the 6-311G* basis set. Calculations on AlNC and AlCl were performed using both MP2/6-311G* geometry optimized structures as well as the structures deduced from the experimental rotational constants. The experimental AlCl bond length, r_e(Al,Cl) = 2.1298 Å,[71] is quite close to the MP2/6-311G* bond length, and as a result, the chemical shielding parameters are quite similar. However, for AlNC the experimental value determined for r_{o}(Al,N), 1.849 Å,[13] is significantly different from the theoretical equilibrium bond length.

In comparison to the span calculated for AlCl (Ω = 487.6 ppm, RHF/6-311G*), a very large span is predicted for AlH (Ω = 986.6 ppm), and a smaller span is calculated for AlF (Ω = 329.8 ppm). It is possible to qualitatively rationalize the increasing span (i.e., Ω(AlF) < Ω(AlCl) < Ω(AlH)) in terms

TABLE 3: Experimental and Calculated Aluminum-27 Chemical Shielding Parameters for a Series of Simple Al-Containing Molecules

		6-31G*		6-311G*(*)[a]	
	experimental (SR data)[b]	RHF[c]	DFT (B3LYP)[d]	RHF[c]	DFT (B3LYP)[d]
		AlNC[e]			
$\sigma_{\parallel}$ (ppm)	789.9	791.6	791.6	791.6	792.3
$\sigma_{\perp}$ (ppm)	384.3	460.5	422.6	414.9	374.9
σ_{iso} (ppm)	519.5	570.9	545.6	540.5	514.0
Ω (ppm)	405.6	331.1	369.0	376.7	417.4
		AlNC[f]			
$\sigma_{\parallel}$ (ppm)	789.9	791.9	791.8	791.9	792.6
$\sigma_{\perp}$ (ppm)	384.3	442.7	404.6	394.0	354.1
σ_{iso} (ppm)	519.5	559.1	533.7	526.7	500.2
Ω (ppm)	405.6	349.2	387.1	397.9	438.5
		AlCl[e]			
$\sigma_{\parallel}$ (ppm)	789.9	793.7	793.8	793.7	794.6
$\sigma_{\perp}$(ppm)	312.5	373.8	330.0	309.0	257.6
σ_{iso} (ppm)	471.6	513.8	484.6	470.6	436.7
Ω (ppm)	477.4	419.9	463.8	484.7	536.8
		AlCl[g]			
$\sigma_{\parallel}$ (ppm)	789.9	793.8	793.9	793.8	794.7
$\sigma_{\perp}$ (ppm)	312.5	371.7	328.5	306.2	255.6
σ_{iso} (ppm)	471.6	512.4	483.6	468.7	435.3
Ω (ppm)	477.4	422.1	465.4	487.6	539.1
		AlH[h]			
$\sigma_{\parallel}$ (ppm)		787.3	787.2	787.3	787.9
$\sigma_{\perp}$ (ppm)		−84.8	−164.5	−199.3	−292.0
σ_{iso} (ppm)		205.9	152.7	129.6	68.0
Ω (ppm)		872.1	951.7	986.6	1079.9
		AlF[i]			
$\sigma_{\parallel}$ (ppm)		791.8	792.2	791.9	793.0
$\sigma_{\perp}$ (ppm)		501.6	457.4	462.0	417.9
σ_{iso} (ppm)		598.3	569.0	572.0	542.9
Ω (ppm)		290.2	334.7	329.8	375.1
		AlH_4^- [e,j]			
σ_{iso} (ppm)		561.9	542.8	518.3	492.5
Ω (ppm)		0	0	0	0

[a] Note that for hydrogen-containing systems, 6-31G** and 6-311G** basis sets were used so as to include polarization functions on the hydrogen atoms. [b] The principal components of the ^{27}Al chemical shielding tensors are calculated from known nuclear spin-rotation coupling constants for AlNC and AlCl. Errors in these components are given in the text. [c] Restricted Hartree−Fock GIAO shielding calculation using Gaussian 94. [d] Density functional theory calculation using Becke's three-parameter hybrid method using the Lee et al. correlation functional (B3LYP), also using Gaussian 94. [e] Calculations performed on the MP2/6-311G*(*) geometry optimized structures: r(Al,Cl) = 2.1364 Å, r(Al,N) = 1.8802 Å, r(N,C) = 1.1936 Å, and in AlH_4^-, r(Al,H) = 1.6377 Å. [f] Calculations performed on the AlNC molecule using the experimentally determined Al,N and N,C bond lengths, r(Al,N) = 1.849 Å and r(N,C) = 1.171 Å.[13] [g] Calculations performed on AlCl using the experimentally determined bond length, r(Al,Cl) = 2.1298 Å.[71] [h] Calculations performed on AlH using the experimentally determined bond length, r(Al,H) = 1.6453622 Å.[72c] [i] Calculations performed on AlF using the experimental bond length, r(Al,F) = 1.65436 Å.[73] [j] Due to the high symmetry of this system (T_d), there is no chemical shielding anisotropy. Isotropic chemical shielding values are reported.

of magnetic dipole allowed $\sigma \rightarrow \pi^*$ mixing. From simple RHF Mulliken population and natural bond order analyses[74] with both the 6-31G* and 6-311G* basis sets, several interesting results are noted. In all three molecules, the HOMO and LUMO are σ and π^* molecular orbitals, respectively, with large contributions from the valence shell atomic orbitals of the aluminum atom. The energy difference between the HOMO and LUMO decreases in a linear fashion with respect to chemical shielding (i.e., ΔE(Al,F) > ΔE(Al,Cl) > ΔE(Al,H)).[16d] The relationship between the CS and ΔE stems from the dependence of the paramagnetic shielding contribution on the excited electronic states. Thus, the smaller the separation is between the HOMO and LUMO, the larger the paramagnetic shielding contribution, and correspondingly, the larger the CSA. It is also interesting to note that the ionic/covalent character of the molecules follows the same trend, with population analyses indicating that AlF is essentially an ionically bound species, whereas AlCl and AlH have increasingly covalent bonding character.[75] In fact, the electric dipole moment of AlH is $\mu_e = -0.10$ D.[76]

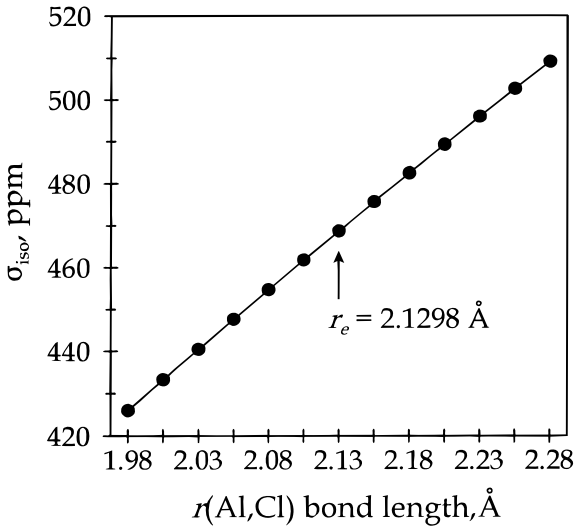

Figure 8. Plot showing the linear relationship between the isotropic chemical shielding and the bond length in aluminum chloride. Calculations were carried out using the RHF/GIAO method with the 6-311G* basis set, decrementing r(Al,Cl) in 0.025 Å steps from the equilibrium bond length, r_e = 2.1298 Å.

Finally, experimental and theoretical values of $C_Q(^{27}Al)$ for all four systems are presented in Table 4. Values of C_Q obtained from RHF, DFT, and MP2 calculations conducted using the 6-311G*(*) basis set are quite close to experimental values with the exception of C_Q in AlH.[77] Nuclear quadrupole coupling constants vary due to distortions in molecular geometry that are dependent on the vibrational state of the molecule, isotopic substitution, and intermolecular interactions.[78] However, MP2/6-311G** calculations of $C_Q(^{27}Al)$ in AlH for varying bond lengths near r_e yield $\partial C_Q/\partial r \simeq -50$ MHz/Å, indicating that rovibrational averaging cannot account for the difference in the experimental and theoretical C_Q (vide infra). Elimination of the polarization functions on the hydrogen atom has little effect on the calculated results (i.e., MP2/6-311G* calculations). Possible reasons for the discrepancy between experimental and calculated $C_Q(^{27}Al)$ in AlH will be discussed elsewhere.

Rovibrational Corrections for the Aluminum Chemical Shielding of AlCl. The magnetic shielding experienced by a nucleus in a molecule is known to depend on subtle changes in molecular geometry. For example, the temperature dependence of nuclear magnetic shielding constants arises from varying populations of different allowed rotational and vibrational states.[79,80] Similarly, isotope effects on magnetic shielding arise because of the different "average" structures of isotopomers.[81] The theoretical sensitivity of aluminum shielding to variations in bond length in aluminum chloride is shown in Figure 8. First, it is clear that the derivative, $\partial\sigma/\partial r$, is positive, 278 ppm/Å at r_e . Positive values of $\partial\sigma/\partial r$ have also been calculated for aluminum(III) hydride,[82] but for group 14, 15, 16, and 17 hydrides this derivative is negative on the basis of theory and experiment.[82,83] Second, from the data shown in Figure 8, one

TABLE 4: Experimental and Calculated Aluminum-27 Nuclear Quadrupole Coupling Constants for a Series of Linear Al-Containing Molecules[a]

		6-31G*			6-311G*		
	experimental	RHF	B3LYP	MP2	RHF	B3LYP	MP2
AlH	−36.72(33)[b]	−40.24	−41.13	−39.54	−50.17	−51.78	−49.46
AlF	−37.6(1.0)[c]	−30.7	−29.9	−30.1	−37.7	−36.4	−37.0
AlCl	−29.2(2.0)[c], −30.4081(27)[d]	−25.90	−24.08	−24.07	−32.93	−31.60	−30.84
AlNC	−35.6268(16)[e]	−30.50	−30.14	−29.26	−38.21	−38.17	−36.69

[a] All C_Q reported in MHz. All values for $\eta = 0$. For all molecules, experimentally determined bond lengths were applied in the calculations (see Table 3 for details). [b] Ref 77. [c] Ref 71. [d] Ref 15. [e] Ref 14.

can estimate the rovibrational correction of the aluminum shielding constant, using the following expressions:

$$\langle\sigma\rangle_{v,J} - \sigma_e \simeq \left(\frac{\partial\sigma}{\partial\xi}\right)_{\xi=0}\langle\xi\rangle_{v,J} + \left(\frac{1}{2}\right)\left(\frac{\partial^2\sigma}{\partial\xi^2}\right)_{\xi=0}\langle\xi^2\rangle_{v,J} \quad (10)$$

where $\xi = (r - r_e)/r_e$ and the average values $\langle\xi\rangle_{v,J}$ and $\langle\xi^2\rangle_{v,J}$ are defined as follows:[79,80]

$$\langle\xi\rangle_{v,J} = -3a_1\left(\frac{B_e}{\omega_e}\right)\left[\frac{1}{2}\coth(hc\omega_e/2kT)\right] + 4(kT/hcB_e)\left(\frac{B_e}{\omega_e}\right)^2 \quad (11)$$

$$\langle\xi^2\rangle_{v,J} = [\coth(hc\omega_e/2kT)]\left(\frac{B_e}{\omega_e}\right) \quad (12)$$

where a_1 is the cubic force constant,

$$-a_1 = \frac{\alpha_e\omega_e}{6B_e^2} + 1 \quad (13)$$

For AlCl, $a_1 = -3.1735$.[84] Analysis of the data shown in Figure 8 indicates that $(\partial\sigma/\partial\xi)_{\xi=0} = 592$ ppm and $(\partial^2\sigma/\partial\xi^2)_{\xi=0} = -452$ ppm. Using the above expressions with $B_e = 0.243942$ cm^{-1} and $\omega_e = 481.67$ cm^{-1} [84] yields $\langle\sigma\rangle_{v,J} - \sigma_e = 2.12$ ppm. Given that $\sigma_{||}$ is essentially independent of r, $\sigma_{||}$ will be independent of temperature, and thus $\langle\sigma_\perp\rangle_{v,J} - \sigma_{\perp,e} = 3.18$ ppm. In summary, the theoretical calculations indicate that the rovibrational averaging effects on aluminum shielding are relatively small and are not responsible for the discrepancies between theory and experiment.

Conclusions

Several examples in the two extremes of ^{27}Al CSA have been presented in this paper. Very small spans of 3.8, 6.7, and 9.0 ppm were obtained for the six-coordinate compounds Al(acac)$_3$, Al(TMHD)$_3$, and Al(trop)$_3$ from solid-state ^{27}Al NMR spectra. Large spans of 406 and 477 ppm in AlNC and AlCl were calculated from ^{27}Al nuclear spin-rotation constants obtained from microwave spectra. Though these results increase the number of reported cases of ^{27}Al CSA to eight, we believe that more work should be done characterizing ^{27}Al CS tensors in order to better understand the nature of the chemical shielding interaction in aluminum and other group 13 elements. In terms of obtaining CS tensors with small CSAs from solid-state NMR spectra, it is clearly advantageous to obtain spectra at high magnetic fields. As well, it has been shown that it is beneficial to combine experimental and theoretical data to fully characterize chemical shielding orientations in the molecular frame. Although ambiguity remains in the exact orientation of the CS and EFG tensors in the molecular frames of Al(acac)$_3$, Al(TMHD)$_3$, and Al(trop)$_3$, the relative CS and EFG orientations along with the orientations of the largest components of the EFG tensors in the molecular frame have been determined. Comparison of the CS tensors and EFG parameters in simple linear molecules obtained from both experiment and theory reveal that it is possible to obtain relatively accurate theoretical CS parameters for simple molecules using present-day computational methods.

Acknowledgment. We thank the Natural Sciences and Engineering Research Council (NSERC) of Canada for funding (R.E.W.) and the Atlantic Regional Magnetic Resonance Centre (ARMRC) for the solid-state NMR facilities. R.W.S. thanks the Killam Foundation and the Walter C. Sumner Foundation for graduate fellowships. R.E.W. thanks the Canada Council for a Killam Research Fellowship. We thank Richard Warren for preparing the Al(trop)$_3$ complex; Elinor Cameron for extensive crystal database searches; and Guy Bernard, Myrlene Gee, and Scott Kroeker for many helpful comments. We also are indebted to Dr. Klaus Eichele for his development of the WSOLIDS software utilized in our laboratory.

References and Notes

(1) Smith, M. E. *Appl. Magn. Reson.* **1993**, *4*, 1.
(2) (a) Sundholm, D.; Olsen, J. *Phys. Rev. Lett.* **1993**, *A47*, 2672. (b) Pyykkö, P. *Z. Naturforsch.* **1992**, *47A*, 189.
(3) Bastow, T. J. *Z. Naturforsch.* **1993**, *49A*, 320.
(4) Klinowski, J. *Anal. Chim. Acta* **1993**, *283*, 929.
(5) Alemany, L. B. *Appl. Magn. Reson.* **1993**, *4*, 179.
(6) Delpuech, J. J. *NMR of Newly Accessible Nuclei—Volume 2: Chemically and Biochemically Important Elements*; Laszlo, P., Ed.; Academic Press: New York, 1983; pp 153−195.
(7) Akitt, J. W. *Prog. NMR Spectrosc.* **1989**, *21*, 1.
(8) Samoson, A.; Sarv, P.; van Braam Houckgeest, J. P.; Kraushaar-Czarnetzki, B. *Appl. Magn. Reson.* **1993**, *4*, 171.
(9) Vosegaard, T.; Jakobsen, H. J. *J. Magn. Reson.* **1997**, *128*, 135.
(10) Schurko, R. W.; Wasylishen, R. E.; Phillips, A. D. *J. Magn. Reson.* **1998**, *133*, 388.
(11) For a review on the Knight shift and references to original articles, see: Knight, W. D.; Kobayashi, S. *Encyclopedia of NMR*; Grant, D. M., Harris, R. K., Eds.; John Wiley & Sons: Chichester, England, 1996; pp 2673−2679.
(12) (a) Smith, M. E.; Gibson, M. A.; Forwood, C. T.; Bastow, T. J. *Philos. Magn. A* **1996**, *74*, 791. (b) Bastow, T. J.; Smith, M. E.; West, G. W. *J. Phys. Condens. Matter* **1997**, *9*, 6085.
(13) Robinson, J. S.; Apponi, A. J.; Ziurys, L. M. *Chem. Phys. Lett.* **1997**, *278*, 1.
(14) Walker, K. A.; Gerry, M. C. L. *Chem. Phys. Lett.* **1997**, *278*, 9.
(15) Hensel, K. D.; Styger, C.; Jäger, W.; Merer, A. J.; Gerry, M. C. L. *J. Chem. Phys.* **1993**, *99*, 3320.
(16) (a) Sykes, D.; Kubicki, J. D.; Farrar, T. C. *J. Phys. Chem. A* **1997**, *101*, 2715. (b) Nakatsuji, H.; Hada, M.; Tejima, T.; Nakajima, T.; Sugimoto, M. *Chem. Phys. Lett.* **1996**, *249*, 284. (c) Schneider, U.; Ahlrichs, R. *Chem. Phys. Lett.* **1994**, *226*, 491. (d) Gauss, J.; Schneider, U.; Ahlrichs, R.; Dohmeier, C.; Schnöckel, H. *J. Am. Chem. Soc.* **1993**, *115*, 2402. (e) Kanzaki, M. *J. Ceram. Soc. Jpn.* **1997**, *105*, 91. (f) Tossell, J. A. *Nuclear Magnetic Shieldings and Molecular Structure*; Tossell, J. A., Ed.; Kluwer Academic Publishers: Dordrecht, 1993; pp 279−296. (g) Laws, E. A.; Stevens, R. M.; Lipscomb, W. N. *J. Chem. Phys.* **1971**, *54*, 4269. (h) O'Reilly, D. E. *J. Chem. Phys.* **1960**, *32*, 1007.
(17) Höller, R.; Lischka, H. *Mol. Phys.* **1980**, *41*, 1041.

(18) Muetterties, E. L.; Wright, C. M. *J. Am. Chem. Soc.* **1964**, *86*, 5132.
(19) Alderman, D. W.; Solum, M. S.; Grant, D. M. *J. Chem. Phys.* **1986**, *84*, 3717.
(20) Frisch, M. J.; Trucks, G. W.; Schlegel, H. B.; Gill, P. M. W.; Johnson, B. G.; Robb, M. A.; Cheeseman, J. R.; Keith, T.; Petersson, G. A.; Montgomery, J. A.; Raghavachari, K.; Al-Laham, M. A.; Zakrewski, V. G.; Ortiz, J. V.; Foresman, J. B.; Cioslowski, J.; Stefanov, B. B.; Nanayakkara, A.; Challacombe, M.; Peng, C. Y.; Ayala, P. Y.; Chen, W.; Wong, M. W.; Andres, J. L.; Replogle, E. S.; Gomperts, R.; Martin, R. L.; Fox, D. J.; Binkley, J. S.; Defrees, D. J.; Baker, J.; Stewart, J. P.; Head-Gordon, M.; Gonzalez, C.; Pople, J. A. *Gaussian 94, Revision B.2*; Gaussian, Inc.: Pittsburgh, PA, 1995.
(21) (a) Ditchfield, R. *Mol. Phys.* **1974**, *27*, 789. (b) Wolinski, K.; Hinton, J. F.; Pulay, P. *J. Am. Chem. Soc.* **1990**, *112*, 8251 and references therein.
(22) Becke, A. D. *J. Chem. Phys.* **1993**, *98*, 5648.
(23) Lee, C.; Yang, W.; Parr, R. G. *Phys. Rev. B* **1988**, *37*, 785.
(24) Nöth, H. *Z. Naturforsch.* **1980**, *35B*, 119.
(25) Tarasov, V. P.; Kirakosyan, G. A. *Russ. J. Inorg. Chem.* **1997**, *42*, 1223.
(26) Brown, R. D.; Head-Gordon, M. P. *Mol. Phys.* **1987**, *61*, 1183. (b) Cummins, P. L.; Bacskay, G. B.; Hush, N. S. *Mol. Phys.* **1987**, *62*, 193.
(27) (a) Andrew, E. R.; Newing, R. A. *Proc. Phys. Soc. (London)* **1958**, *72*, 959. (b) Andrew, E. R.; Bradbury, A.; Eades, R. G. *Nature* **1958**, *182*, 1659. (c) Lowe, I. J. *Phys. Rev. Lett.* **1959**, *2*, 285.
(28) Samoson, A.; Kundla, E.; Lippmaa, E. *J. Magn. Reson.* **1982**, *49*, 350.
(29) Taulelle, F. *Multinuclear Magnetic Resonance in Liquids and Solids—Chemical Applications*; NATO ASI Series 322; Granger, P., Harris, R. K., Eds.; Kluwer Academic Publishers: Dordrecht, 1990; pp 393−407.
(30) Amoureux, J. P.; Fernandez, C.; Granger, P. *Multinuclear Magnetic Resonance in Liquids and Solids—Chemical Applications*; NATO ASI Series 322; Granger, P., Harris, R. K., Eds.; Kluwer Academic Publishers: Dordrecht, 1990; pp 409−424.
(31) Freude, D.; Haase, J. *NMR Basic Principles and Progress*; Diehl, P., Fluck, E., Günther, H., Kosfeld, R., Seelig, J., Eds.; Springer-Verlag: Berlin, 1993; Vol. 29, pp 1−90.
(32) Barrie, P. J. *Chem. Phys. Lett.* **1993**, *208*, 486.
(33) Dechter, J. J.; Henriksson, U.; Kowalewski, J.; Nilsson, A.-C. *J. Magn. Reson.* **1982**, *48*, 503.
(34) Cotton, F. A.; Wilkinson, G. *Advanced Inorganic Chemistry*, 4th ed.; John Wiley & Sons: New York, 1980; pp 166−170.
(35) Muetterties, E. L.; Guggenberger, L. J. *J. Am. Chem. Soc.* **1972**, *94*, 8046.
(36) (a) Rahman, A.; Nizamuddin Ahmed, S.; Khair, M. A.; Zangrando, E.; Randaccio, L. *J. Bangladesh. Acad. Sci.* **1990**, *14*, 161. (b) Hon, P. K.; Pfluger, C. E. *J. Coord. Chem.* **1973**, *3*, 67. (c) McClelland, B. W. *Acta Crystallogr.* **1975**, *B31*, 2496.
(37) Baugher, J. F.; Taylor, P. C.; Oja, T.; Bray, P. J. *J. Chem. Phys.* **1969**, *50*, 4914.
(38) Taylor, P. C.; Baugher, J. F.; Kriz, H. M. *Chem. Rev.* **1975**, *75*, 203.
(39) Cheng, J. T.; Edwards, J. C.; Ellis, P. D. *J. Phys. Chem.* **1990**, *94*, 553.
(40) Power, W. P.; Wasylishen, R. E.; Mooibroek, S.; Pettitt, B. A.; Danchura, W. *J. Phys. Chem.* **1990**, *94*, 591.
(41) Koons, J. M.; Hughes, E.; Cho, H. M.; Ellis, P. D. *J. Magn. Reson. A* **1995**, *114*, 12.
(42) Mason, J. *Solid State Nucl. Magn. Reson.* **1993**, *2*, 285.
(43) (a) Harris, R. K. *Solid State Nucl. Magn. Reson.* **1998**, *10*, 177. (b) Jameson, C. J. *Solid State Nucl. Magn. Reson.* **1998**, *11*, 265.
(44) Zare, R. N. *Angular Momentum—Understanding Spatial Aspects in Chemistry and Physics*; John Wiley & Sons: New York, 1988.
(45) Eichele, K.; Wasylishen, R. E.; Nelson, J. H. *J. Phys. Chem. A* **1997**, *101*, 5463.
(46) Freude, D.; Haase, J. *NMR Basic Principles and Progress*; Diehl, P., Fluck, E., Günther, H., Kosfeld, R., Seelig, J., Eds.; Springer-Verlag: Berlin, 1993; Vol. 29, p 1.
(47) Weil, J. A.; Buch, T.; Clapp, J. E. *Adv. Magn. Reson.* **1973**, *6*, 183.
(48) Reynhardt, E. C. *J. Phys. C: Solid State Phys.* **1974**, *7*, 4135.
(49) Eichele, K.; Chan, J. C. C.; Wasylishen, R. E.; Britten, J. F. *J. Phys. Chem. A* **1997**, *101*, 5423.
(50) Veeman, W. S. *Prog. NMR Spectrosc.* **1984**, *16*, 193.
(51) Grant, D. M. *Encyclopedia of Nuclear Magnetic Resonance*; Grant, D. M., Harris, R. K., Eds.; John Wiley & Sons: Chichester, U.K., 1996; pp 1298−1321.
(52) Sherwood, M. H. *Encyclopedia of Nuclear Magnetic Resonance*; Grant, D. M.,Harris, R. K., Eds.; John Wiley & Sons: Chichester, U.K., 1996; pp 1322−1330.
(53) Grant, D. M.; Facelli, J. C.; Alderman, D. W.; Sherwood, M. H. *Nuclear Magnetic Shieldings and Molecular Structure*; Tossell, J. A., Ed.; Kluwer Academic Publishers: Dordrecht, 1993; pp 367−384 and references therein.
(54) Ditchfield, R. *Critical Evaluation of Chemical and Physical Structural Information*; Lide, D. R., Paul, M. A., Eds.; National Academy of Sciences: Washington, DC, 1974; pp 565−590.
(55) Segleken, W. G.; Torrey, H. C. *Phys. Rev.* **1955**, *98*, 1537.
(56) Dewar, M. J. S.; Patterson, D. B.; Simpson, W. I. *J. Chem. Soc., Dalton Trans.* **1973**, 2381.
(57) Slichter, C. P. *Principles of Magnetic Resonance*, 3rd ed.; Springer-Verlag: New York, 1990; pp 500−502.
(58) (a) de Dios, A. C. *J. Prog. NMR Spectrosc.* **1996**, *29*, 229. (b) Fukui, H. *Prog. NMR Spectrosc.* **1997**, *31*, 317.
(59) (a) Pernpointner, M.; Seth, M.; Schwerdtfeger, P. *J. Chem. Phys.* **1998**, *108*, 6722. (b) Pernpointner, M.; Schwerdtfeger, P.; Hess, B. A. *J. Chem. Phys.* **1998**, *108*, 6739.
(60) Pyykkö, P.; Seth, M. *Theor. Chem. Acc.* **1997**, *96*, 92.
(61) Jameson, C. J.; Mason, J. *Multinuclear NMR*; Mason, J., Ed.; Plenum Press: New York, 1987; pp 51−83.
(62) Jameson, C. J. *Encyclopedia of Nuclear Magnetic Resonance*; Grant, D. M., Harris, R. K., Eds.; John Wiley & Sons: Chichester, U.K., 1996; pp 1273−1281.
(63) Ramsey, N. F. *Phys. Rev.* **1950**, *78*, 699.
(64) (a) Christiansen, O.; Gauss, J.; Stanton, J. F. *Chem. Phys. Lett.* **1997**, *266*, 53. (b) Chesnut, D. B.; Byrd, E. F. C. *Heteratom Chem.* **1996**, *7*, 307. (c) Gauss, J.; Ruud, K. *Int. J. Quantum Chem.* **1995**, *29*, 437.
(65) (a) Schreckenbach, G.; Dickson, R. M.; Ruiz-Morales, Y.; Ziegler, T. *Chemical Applications of Density-Functional Theory*; Laird, B. B., Ross, R. B., Ziegler, T., Eds.; American Chemical Society: Washington, DC, 1996; p 328. (b) Rauhut, G.; Puyear, S.; Wolinski, K.; Pulay, P. *J. Phys. Chem.* **1996**, *100*, 6310. (c) Malkin, V. G.; Malkina, O. L.; Casida, M. E.; Salahub, D. R. *J. Am. Chem. Soc.* **1994**, *116*, 5898.
(66) Frisch, M. J.; Frisch, A.; Foresman, J. B. *Gaussian 94 User's Reference*; Gaussian Inc.: Pittsburgh, 1996; pp 109−110.
(67) (a) Flygare, W. H. *Chem. Rev.* **1974**, *74*, 653. (b) Gierke, T. D.; Flygare, W. H. *J. Am. Chem. Soc.* **1972**, *94*, 7277. (c) Flygare, W. H.; Goodisman, J. *J. Chem. Phys.* **1968**, *49*, 3122.
(68) Malli, G.; Froese, C. *Int. J. Quantum Chem.* **1967**, IS, 95.
(69) (a) Müller, H. S. P.; Gerry, M. C. L. *J. Chem. Phys.* **1995**, *103*, 577. (b) Baker, M. R.; Anderson, C. H.; Ramsey, N. F. *Phys. Rev.* **1964**, *133*, A1533.
(70) Gatehouse, B.; Müller, H. S. P.; Gerry, M. C. L. *J. Chem. Phys.* **1997**, *106*, 6916 and references therein.
(71) Lide, D. R. *J. Chem. Phys.* **1965**, *42*, 1013.
(72) (a) Holst, W.; Hulthén, E. *Z. Physik* **1934**, *90*, 712. (b) Deutsch, J. L.; Neil, W. S.; Ramsay, D. A. *J. Mol. Spectrosc.* **1987**, *125*, 115. (c) White, J. B.; Dulick, M.; Bernath, P. F. *J. Chem. Phys.* **1993**, *99*, 8371. Calculation using bond length from c shown in Table 3.
(73) (a) Lide, D. R. *J. Chem. Phys.* **1963**, *38*, 2027. (b) Wyse, F. C.; Gordy, W. *J. Chem. Phys.* **1970**, *52*, 3887.
(74) Carpenter, J. F.; Weinhold, F. *J. Mol. Struct. (THEOCHEM)* **1988**, *169*, 41 and references therein.
(75) Gordy, W.; Cook, R. L. *Microwave Molecular Spectra*; John Wiley & Sons: New York, 1984; p 756.
(76) Tipping, R. H.; Pineiro, A. L.; Chackerian, C. *Astrophys. J.* **1987**, *323*, 810.
(77) Goto, M.; Saito S. *Astrophys. J. Lett.* **1995**, *452*, 147.
(78) Lucken, E. A. *Adv. Nucl. Quadrupole Reson.* **1983**, *5*, 83.
(79) Buckingham, A. D. *J. Chem. Phys.* **1962**, *36*, 3096.
(80) Jameson, C. J. *J. Chem. Phys.* **1977**, *66*, 4977.
(81) Jameson, C. J. *J. Chem. Phys.* **1977**, *66*, 4983.
(82) Chesnut, D. B. *Chem. Phys. Lett.* **1986**, *110*, 415.
(83) (a) Jameson, C. J.; de Dios, A. C. *J. Chem. Phys.* **1993**, *98*, 2208. (b) de Dios, A. C.; Jameson, C. J. *Annu. Rep. NMR Spectrosc.* **1994**, *29*, 1.
(84) Wyse, F. C.; Gordy, W. *J. Chem. Phys.* **1972**, *56*, 2130.